



# Designing a tuned-shunt electrodynamic metamaterial in the presence of uncertainties.

Lawrence Singleton<sup>1</sup>, Jordan Cheer and Stephen Daley  
Institute of Sound and Vibration Research  
University of Southampton, University Road, Southampton, SO17 1BJ, UK

## ABSTRACT

*Resonant structural vibrations are a common source of disruptive noise, and suppressing these vibrations is often the most direct way to reduce the noise levels. Elastic metamaterials (EMMs) consist of distributed resonant substructures, at a scale which is small compared to the wavelength of vibration. This allows these materials to be used in applications where space is limited, and more traditional vibration suppression techniques would be impractical. Tuned resonators can be designed through selection of geometry or material properties, but an alternative approach, which requires significantly less prototyping, is through the use of shunted electrodynamic inertial actuators. In this paper, a novel electrodynamic metamaterial (EDMM) is proposed consisting of an array of mass-produced inertial actuators, each connected to a tuned shunt impedance. It is considered impractical to measure the dynamic and electrical parameters of a large number of actuators, and so the effect of uncertainties in the actuators is investigated on both the performance and the stability of the EDMM.*

## 1. INTRODUCTION

Vibration control is an important aspect of engineering. Structural vibration can cause acoustic disturbance, accelerated wear, or even structural failure. As the conservation of materials and energy becomes more and more important, structures are made thinner and lighter. However, this also results in a structure that is more receptive to vibration. Traditional tuned vibration absorbers are very effective, but present a single concentrated force on a structure, and are often large and heavy. This may not be suited to thin, light structures where a concentrated force may cause deformation or damage, or where space and weight are a premium. Viscoelastic damping layers, while low space, are heavy, and therefore also may not be suited to certain applications.

Elastic metamaterials (EMMs) offer a potential solution to the problem of vibration control, where the application limits weight and size. A metamaterial is a material with a periodic structure, that is able to interact with wavelengths much greater than the periodic scale. EMMs are able to interact with elastic waves in solids. In this case, we are interested in locally resonant EMMs as structural vibration absorbers [1–4]. Vibration absorption occurs when the translational motion of the locally resonant substructures opposes the translational motion of the structure, which occurs around the

---

<sup>1</sup>ls2u17@soton.ac.uk

resonance frequency or frequencies of the substructure [1, 5]. A substructure with multiple resonance frequencies (multiple degrees-of-freedom or multiple resonators), can be used to achieve control over a wider bandwidth or of multiple structural modes [6, 7].

Locally resonant EMMs can be tuned using their geometry, however this requires significant prototyping and modelling, particularly if multiple tuning frequencies are required. An alternative approach is to tune an existing resonator by other means. One such way is by connecting a specific electronic impedance to the terminals of an inertial electrodynamic actuator, also known as shunting [8]. Existing studies in tuned-shunt absorbers do not examine the effect of uncertainties in the electrodynamic devices, instead designing the shunt impedance based on known electromechanical parameters [9–12]. For a small number of devices, measuring the individual parameters is plausible. However, for large arrays, such as you would expect in a metamaterial, this would be impractical. Low-cost inertial actuators are manufactured to quoted tolerances of  $\pm 10\%$  [13, 14], and so the uncertainties need to be taken into account during the design.

This study investigates the effect of realistic actuator uncertainties on the design of a tuned-shunt electrodynamic metamaterial (EDMM). The effect on the uncertainties on the response, the introduction of instabilities in individual actuators, and on a multi-mode EDMM design are considered.

## 2. CHARACTERISATION OF UNCERTAINTY IN AN INERTIAL ELECTRODYNAMIC ACTUATOR

In order to investigate the effects of realistic variation in the parameters of an inertial electrodynamic actuator, this section sets out the results of an experimental investigation, carried out in order to characterise the parameters and the distribution of the variation in a suitable device. Standard techniques were employed to measure the following parameters in a set of 24 Tectonic Audio Labs TEAX09C005-8 miniature inertial actuators [13], shown in Figure 1: moving mass,  $m_r$ ; dynamic stiffness,  $k_r$ ; damping ratio,  $\zeta$ ; magnet transduction coefficient,  $Bl$ ; coil electrical resistance,  $R_e$ ; coil electrical inductance,  $L_e$ .

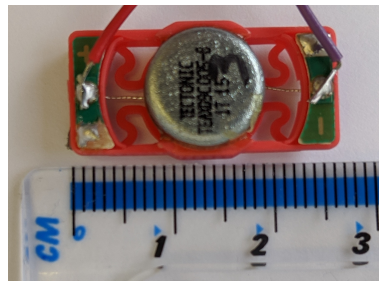


Figure 1: Tectonic Audio Labs TEAX09C005-8.

Figure 2 shows the distribution of each parameter, as histogram plots. Also overlaid is an approximated distribution curve. All parameters can be approximated by a normal distribution, with the exception of the coil electrical resistance,  $R_e$ , which is better approximated by an extreme value distribution. These characterised distributions can next be used to investigate the effects of real-life uncertainties on tuned-shunt design.

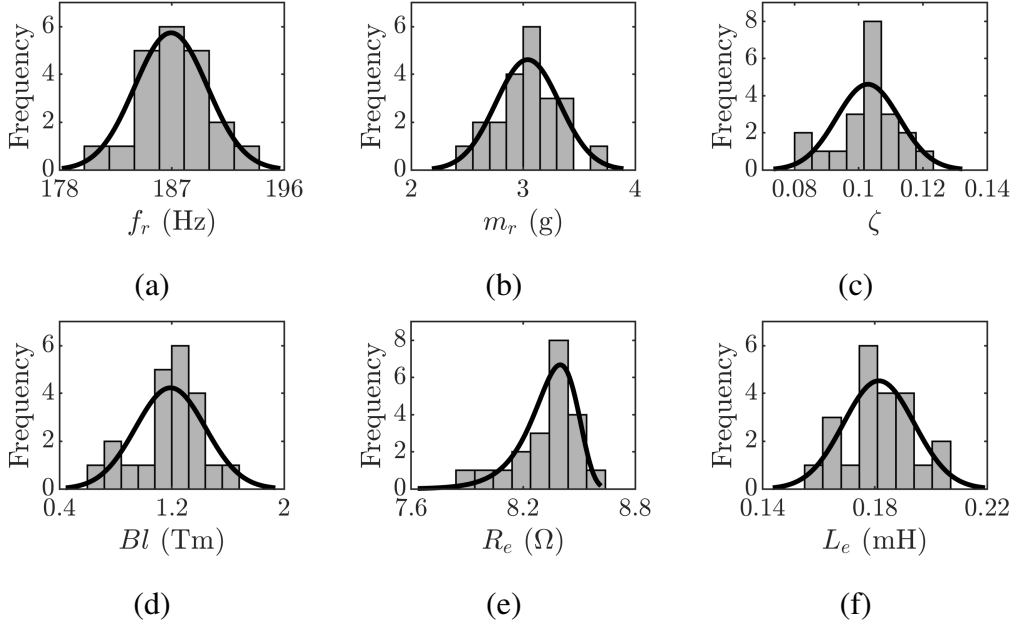


Figure 2: Histograms for. (a)  $f_r$ , (b)  $m_r$ , (c)  $\zeta$ , (d)  $Bl$ , (e)  $R_e$ , (f)  $L_e$ , with overlaid distribution curves.

### 3. THE EFFECT OF SHUNT-IMPEDANCE ON TUNED RESPONSE

Prior to investigating the effect of actuator uncertainties, this section sets out the effect of a shunt impedance on the response of an inertial actuator.

#### 3.1. Modelling a shunted inertial electrodynamic actuator

The effect of a shunt impedance can be evaluated by modelling the inertial actuator as a SDOF mass-spring-damper, with the addition of an electromechanical transduction mechanism between the mass and the base. In an open circuit with the voice coil un-terminated, the effect of the magnet-coil interaction can be disregarded, however, with the voice coil shorted or shunted, the back electromotive force (EMF) transduced when there is a net velocity difference between the base and the mass, presents an additional impedance to motion. The effective mechanical impedance of the electrical part,  $Z_{me}$ , is related to the total electrical impedance of the closed loop,  $Z_{es}$ , by [11]

$$Z_{me} = j\omega \frac{(Bl)^2}{Z_{es}}, \quad (1)$$

A resistor-inductor (RL) tuned-shunt has been demonstrated in the literature [12] and is used in this study. The resulting electromechanical and mechanical-only equivalent models of an RL shunted inertial electrodynamic actuator are shown in Figure 3. The impedance of the actuator base to a displacement, and therefore the impedance presented to an attached structure,  $Z_r$ , can be expressed as

$$Z_r = Z_{sr} \left( 1 - \frac{Z_{sr}}{Z_{sr} + \omega^2 m_r} \right). \quad (2)$$

where

$$Z_{sr} = k_r + j\omega b_r + j\omega \frac{(Bl)^2}{Z_{es}}. \quad (3)$$

#### 3.2. Instabilities in the system

When using negative impedances, there is the potential for the system to become unstable, as energy is put into the system in order to reverse the direction of current flow. The stability of the

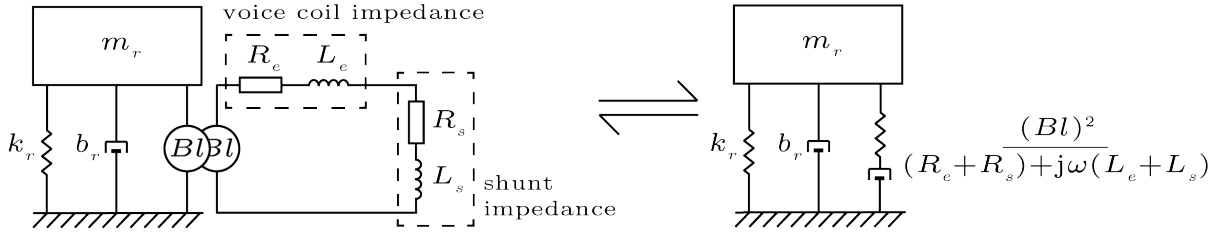


Figure 3: Circuit diagram of actuator in series with resistor,  $R$ .

system is, therefore, a design criterion that must also be considered.

Instabilities can be assessed by considering the poles of the transfer function, which can be shown to fall at the roots of:

$$L_{total}m_r s^3 + (R_{total}m_r + L_{total}b_r)s^2 + (R_{total}b_r + L_{total}k_r + (Bl)^2)s + R_{total}k_r, \quad (4)$$

where  $s = j\omega$ . The system is unstable when the real part of one or more of the three poles is positive, therefore the stability of the system can be assessed by observing the largest real pole. It can be shown numerically that if  $R_{total}$  and  $L_{total}$  have opposite signs, then the system will always be unstable, but other shunt configurations can also lead to instability, and therefore stability can only be assessed by calculating the system poles for a given set of parameters.

### 3.3. Tuning the response using an RL shunt

Figure 4 shows the impedance of the actuator base to a displacement,  $Z_r$ , for different total circuit impedances ( $R_{total} = R_e + R_{shunt}$  and  $L_{total} = L_e + L_{shunt}$ ), with Figure 4.a and 4.b showing the magnitude and phase respectively. This figure demonstrates that a change in resonance frequency is achieved with a change in total circuit inductance and a small total circuit resistance, however it does not show a clear relationship.

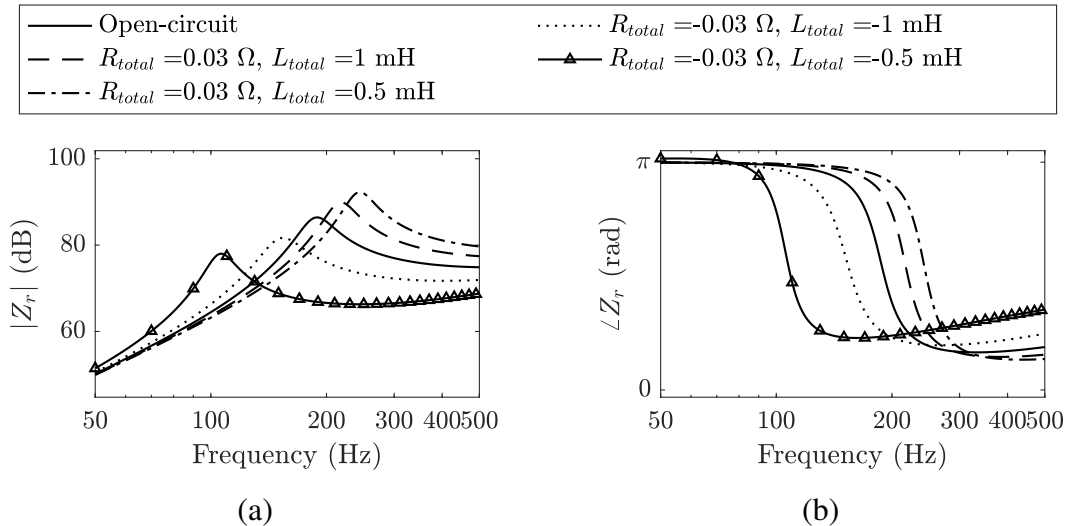


Figure 4: Impedance of the base to displacement,  $Z_r$ , of a tuned-shunt inertial actuator, for different total loop resistance,  $R_{total}$ , and inductance,  $L_{total}$ . (a) magnitude (b) phase.

Figure 5.a and Figure 5.b show the resonance frequency,  $f_r$ , and damping ratio,  $\zeta$ , of a tuned actuator when  $L_{total}$  is varied.  $R_{total}$  remains a constant magnitude, but the sign is changed to match that of  $L_{total}$ . This figure shows that as the magnitude of  $L_{total}$  gets small, the change in resonance

frequency becomes greater, with a negative total inductance resulting in a lower resonance and a positive total inductance an increase. The omitted data at approximately  $-0.5 < L_{total} < 0$ , is where the damping has become so significant that a resonant peak can no longer be distinguished. The effect of varying  $L_{total}$  alone is demonstrated here, but the relationship between this and the shunt resistance,  $R_{shunt}$ , with the response, is more complex.

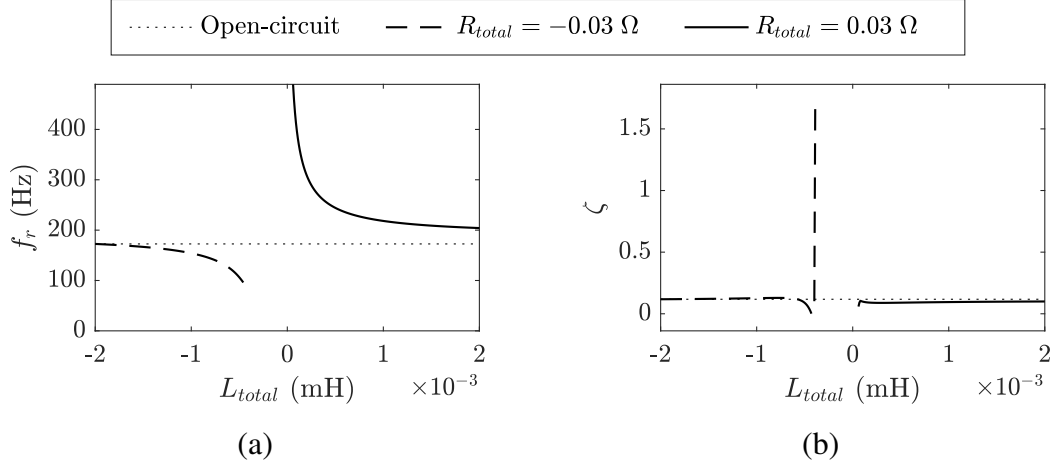


Figure 5: Resonance frequency,  $f_r$ , and damping ratio,  $\zeta$ , of a tuned-shunt inertial actuator, for different total loop resistance,  $R_{total}$ , and inductance,  $L_{total}$ . (a)  $f_r$  (b)  $\zeta$ . The dashed line indicates where  $L_{total}$  and  $R_{total}$  are both negative, the solid line where they are both positive, and the dotted horizontal line is the open-circuit response.

Figure 6 shows the impedance of the actuator base to displacement,  $Z_r$ , with no shunt inductance, so that  $L_{total} = L_e = 0.18$  mH, and various positive total resistances,  $R_{total}$ . Figure 6.a and Figure 6.b show the magnitude and phase of  $Z_r$  respectively, and it appears that for a high total resistance,  $R_{total}$ , the resonance frequency remains very close to the open-circuit, however, at some point between  $R_{total} = 1 \Omega$  and  $R_{total} = 0.3 \Omega$ , the peak in the response suddenly shift up in frequency. This is because when  $R_{total}$  is high compared to  $L_{total}$ , the effect of the inductance is negated, but as it decreases, the inductance has a greater effect, creating a resonance at a different frequency. This is corroborated by Figure 7, which shows the same behaviour but with a tuned-shunt inductance.

The effect of the total resistance,  $R_{total}$ , on the actuator response where  $L_{total} = L_e$ , can be seen more clearly in Figure 8. Figure 8.a and Figure 8.b show the resonance frequency,  $f_r$ , and damping ratio,  $\zeta$ , respectively, for a total resistance in the range  $0 < R_{total} \leq 10$ . It can be seen in Figure 8.a that for  $R_{total} > 4 \Omega$  the resonance frequency closely matches the open-circuit resonance. As  $R_{total}$  decreases below this, the resonance frequency gradually begins to shift up in frequency, until there is a gap in the data at roughly  $0.5 < R_{total} < 1$ . This gap is present because the peak in the response disappears, and a resonance frequency can no longer be determined. The line reappears for  $R_{total} < 0.5 \Omega$ , at 410 Hz, but this time decreasing in frequency to around 325 Hz as  $R_{total}$  tends to 0. Therefore, if the total resistance by design is within the 0-0.5  $\Omega$  range, parametric uncertainty of even  $\pm 5\%$  in  $R_e$  (5% of 8  $\Omega$  is 0.4  $\Omega$ ) would see a significant change in  $f_r$  or even a loss of the resonance peak completely. The effect of  $R_{total}$  on damping ratio,  $\zeta$ , is shown. Figure 8.b shows that as  $R_{total}$  decreases, so does the damping ratio,  $\zeta$ . This is the case until around 1.7  $\Omega$ . It is not clear what causes the irregular peaks and eventual tail off in  $\zeta$  below this, and this will require further investigation. As  $\zeta$  is estimated using the half-power method from the modelled frequency response, when the peak in the response disappears for approximately  $0.5 < R_{total} < 1$ ,  $\zeta$  cannot be estimated. For the range of  $0 < R_{total} < 0.5$ ,  $\zeta$  varies from 0.07 to 0.37. Therefore, as also seen for the resonance frequency,  $f_r$ , for a parametric uncertainty of  $\pm 5\%$  in  $R_e$ , a significant change in  $\zeta$  would be seen.

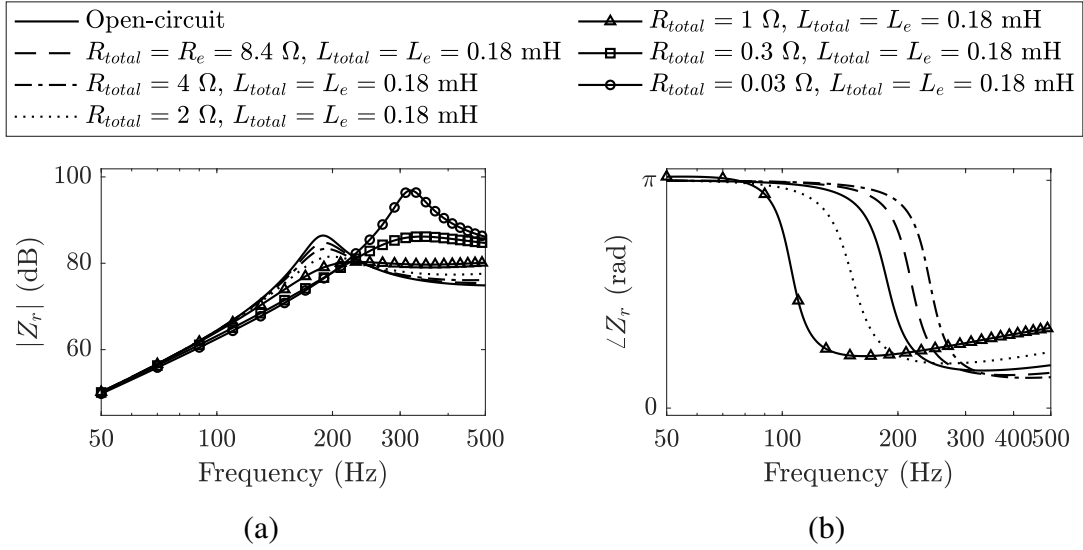


Figure 6: Impedance of the base to displacement,  $Z_r$ , for different total loop resistance,  $R_{total}$ , and no shunt inductance, therefore,  $L_{total} = L_e$ . (a) magnitude, (b) phase.

The results in this section have shown that small variations in the coil impedance from the parameters used in the design process, could achieve very different results. In the following section, the extent of the effect of the realistic variation in the actuator parameters on the behaviour when used as a resonant absorber is explored.

#### 4. THE EFFECT OF UNCERTAINTY ON A TUNED EDMM

This section investigates the effect of the characterised uncertainty on the response of a tuned-shunt inertial actuator. The uncertainty not only has the potential to modify the frequency response such that it deviates from the desired response, but also to result in an unstable system even when the nominal design was stable. The stability in the presence of uncertainty will be considered first, and how that affects the ability to tune the actuators. Then how the uncertainty affects the frequency response will be investigated. Finally, the effect of uncertainty on the performance of a multi-actuator EDMM for absorption of structural vibration is considered.

##### 4.1. Instability in the uncertain system

To evaluate instability, the largest real pole values are calculated by finding the roots to equation 4. Figure 9 shows the largest real pole value,  $\max \Re\{P(H)\}$ , for the characterised uncertainty in each of the electrical parameters individually. Figure 9.a shows that when the actuator is tuned up in frequency, where  $R_{total}$  and  $L_{total}$  are both positive, there is no instability as a result of uncertainty in  $Bl$  alone. However, when the actuator is tuned down in frequency, the system becomes unstable when  $\Re\left\{\frac{(Bl)^2}{R_{total} + j\omega L_{total}}\right\}$  is less than approximately -0.021, a number which is dependent on the mechanical parameters of the actuator. Figure 9.b shows that whether the actuator is tuned up or down in frequency, if there is uncertainty in  $R_e$  that causes  $R_{total}$  to change sign (so that it has a different sign to  $R_{total}$ ), then the system will be unstable. This is expected, since as discussed in Section 2,  $R_{total}$  and  $L_{total}$  must have the same sign to achieve stability. However, it can also be seen from the results in Figure 9.b that when the actuator is tuned down in frequency, the system is unstable when  $\Re\left\{\frac{(Bl)^2}{R_{total} + j\omega L_{total}}\right\}$  is less than approximately -0.021, the same cut-off point seen in Figure 9.a. Figure

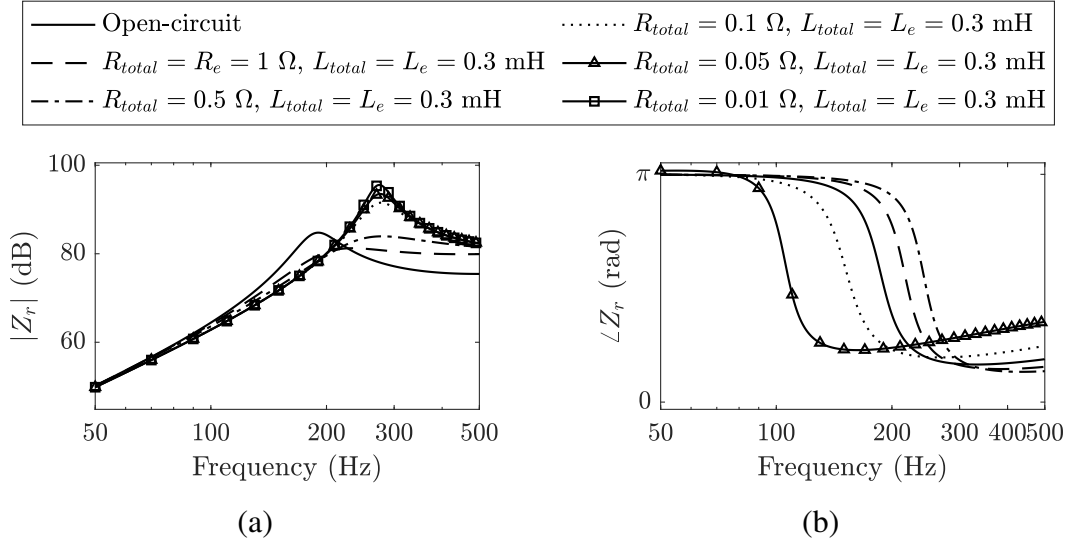


Figure 7: Impedance of the base to displacement,  $Z_r$ , for different total loop resistance,  $R_{total}$ , and tuned total inductance. (a) magnitude, (b) phase.

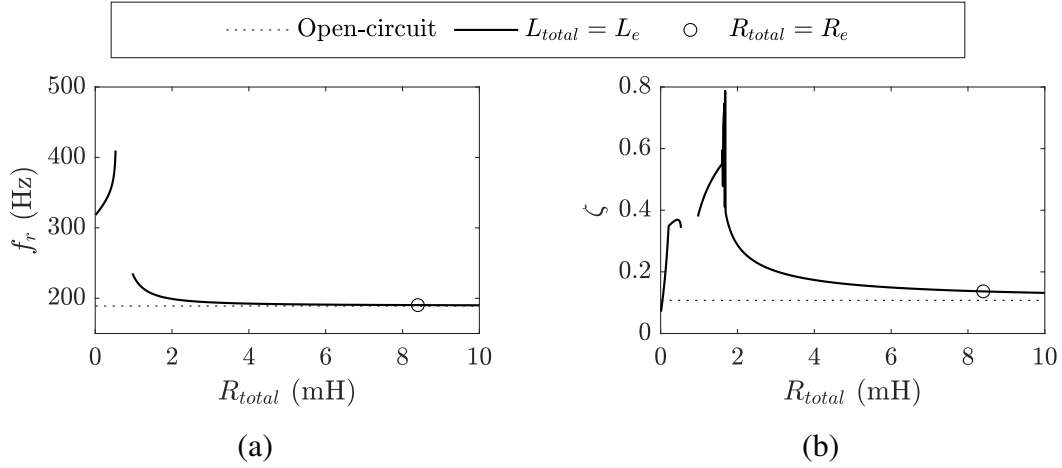


Figure 8: Resonance frequency,  $f_r$ , and damping ratio,  $\zeta$ , for different total loop resistance,  $R_{total}$ , and no shunt inductance, therefore,  $L_{total} = L_e$ . (a)  $f_r$ , (b)  $\zeta$ . The dotted horizontal line indicates the open-circuit value, and the response when  $R_{total} = R_e$ , and therefore there is no impedance to the shunt, is circled.

9.c shows that for the characterised uncertainty in  $L_e$  alone, instabilities are not seen.

It was demonstrated in Section 3 that  $R_{total}$  must be small to achieve a change in resonance frequency, and this makes the uncertainty in  $R_e$  a concern for design as  $R_{total}$  could change sign, causing instability. The nominally designed value for the shunt resistance,  $R_{shunt}$ , and therefore the total resistance,  $R_{total}$ , must be large enough that the uncertainty cannot make it negative. Based on the characterised uncertainty in  $R_e$ , the designed nominal  $R_{total}$  must be greater than  $0.9 \Omega$ , or less than  $0.25 \Omega$ , in order to prevent a change in sign in the presence of uncertainty in  $R_e$ .

With these limitations on  $R_e$  imposed, the actuator response is less affected by the tuned-shunt and the response cannot be tuned to as great an extent, particularly when tuning up in frequency, where the magnitude of the  $R_e$  limitation (dictated by the characterised extreme value distribution of the uncertainty) is greater. However, the effect of the uncertainty is still significant. Figure 10 shows the nominal (solid line) impedance of the actuator base to displacement,  $Z_r$ , and the response

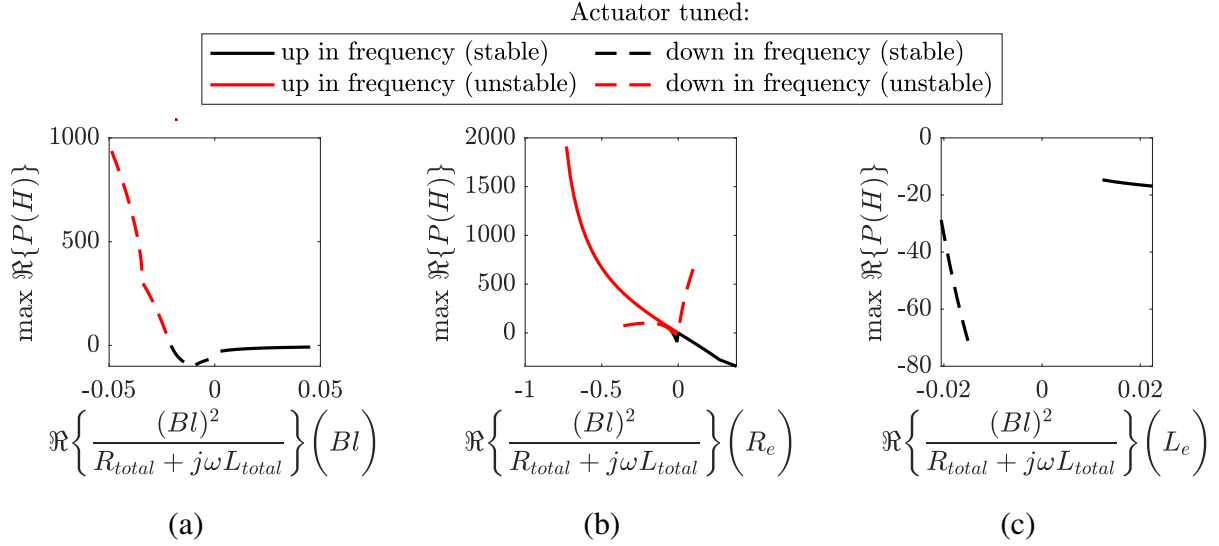


Figure 9: The maximum real part of the transfer function poles,  $\max \Re\{P(H)\}$ , sorted by the real part of the effective electromechanical impedance,  $\Re\left\{\frac{(Bl)^2}{R_{total} + j\omega L_{total}}\right\}$ , with uncertainty in the: (a) transduction coefficient,  $Bl$ , (b) coil resistance,  $R_e$ , (c) coil inductance,  $L_e$ . The solid lines represent the actuator when the resonance is tuned up in frequency, and the dashed lines when the resonance is tuned down in frequency. Instability is highlighted in red.

of realistic actuators, with uncertain mechanical and electrical parameters (dashed line), for: (a) the actuator tuned up in frequency, and (b) the actuator tuned down in frequency, with unstable actuators highlighted in red. It can be seen that there are still instabilities, but only when the actuator is tuned down. This is as expected, since if there is no change in sign of  $R_{total}$  or  $L_{total}$ , the actuator tuned up in frequency will always be stable. Figure 10 shows that there is significant variation in the response of both tuned actuators, due to the uncertainties.

#### 4.2. A tuned EDMM on a structure

In order to visualise the impact of uncertainty in the actuator response in a complete EDMM on a structure, an example is considered. A tuned-shunt EDMM is designed to control four modes of vibration in a cantilever beam. The EDMM consists of a repeated unit cell with four independently tuned and shunted inertial actuators, based on the Tectonic Audio Labs actuator used in the rest of this study. Figure 11.a shows the magnitude of the mean-squared velocity at the tip of the beam,  $|\bar{v}_{tip}^2|$ , for the beam alone (solid line) and with the stable, nominal EDMM attached. It is shown in Figure 11.a that the energy at the four modes has been significantly reduced. However, Figure 11.b shows  $|\bar{v}_{tip}^2|$  for the beam alone compared to several examples of EDMMs with realistic uncertainty in the actuators. Unstable realisations are highlighted in red, and it can be seen that all uncertain cases result in instabilities. As the nominal design limited  $R_{shunt}$  to avoid a change in sign of  $R_{total}$ , these instabilities will be solely due to the actuators tuned down in frequency. Peaks in the tip-velocity response of the treated beam can also be seen at around 140 Hz. These peaks are higher than the modal peaks of the untreated beam, which is highly undesirable for a control treatment.

It has been shown that stability imposes a significant limitation on the tuned value of  $R_{total}$  and therefore the selection of  $R_{shunt}$ , which also limits the ability to tune the actuator both up and down in frequency. If the total resistance,  $R_{total}$ , and total inductance,  $L_{total}$ , have different signs, then instability is guaranteed. Therefore  $|R_{total}|$  is limited to being greater than the maximum possible uncertainty in the coil resistance,  $R_e$ . The performance achievable within this limitation, however, is still to be determined. In the absence of measured coil resistances, improved manufacturing tolerances with

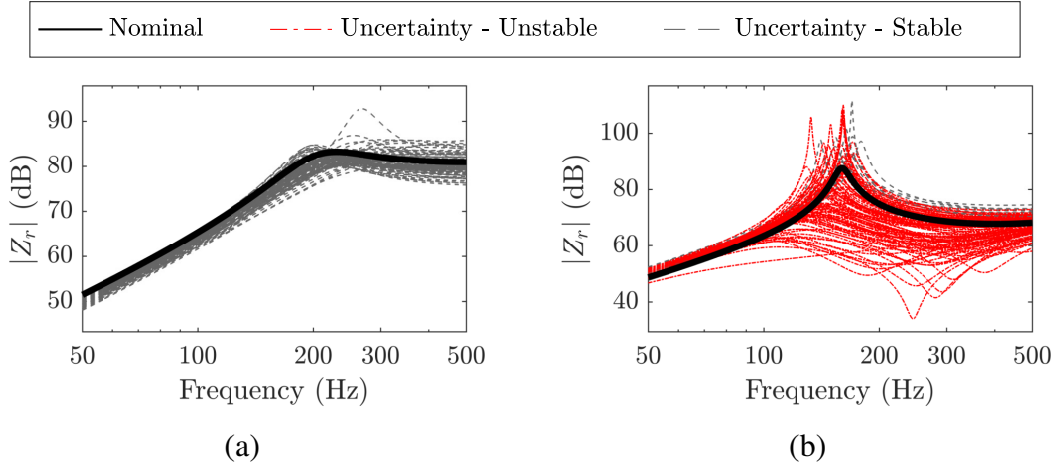


Figure 10: Magnitude of the impedance of the base to displacement,  $Z_r$ , of a tuned-shunt inertial actuator, for: (a) a tuned resonance frequency greater than the open-circuit resonance, (b) a tuned resonance frequency lower than the open-circuit resonance. The actuator with nominal parameters (solid line) is compared to actuators with randomised uncertainties (dashed line). Unstable actuator responses are highlighted in red.

reduced variation in  $R_e$ , would result in greater tuneability. However, even with limiting  $|R_{total}|$ , an EDMM designed based on a nominal actuator response has been shown to be unstable in the presence of uncertainties when actuators are tuned down in frequency. Therefore, the uncertainty must be factored into the design in order to attempt to avoid this.

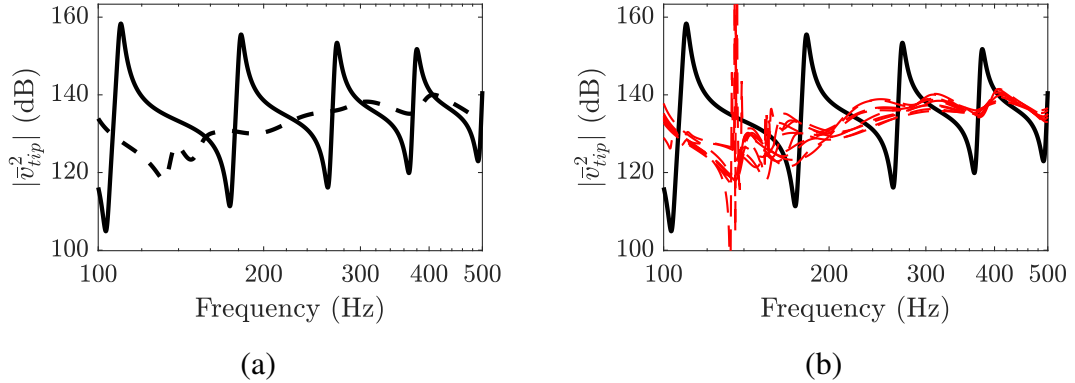


Figure 11: Example of an uncertain EDMM applied to a structure: The mean-squared velocity magnitude of the tip of a cantilever beam,  $|\bar{v}_{tip}^2|$ , with (solid line) and without (dashed line) a tuned-shunt EDMM attached, for: (a) the nominal parameters, (b) randomised actuator uncertainties. Cases with instabilities are highlighted in red.

## 5. CONCLUSIONS

Using an experimental characterisation of the parametric uncertainty in a low-cost miniature electrodynamic actuator, the effect of the uncertainty on its response as a tuned-shunt resonator for use in a tuned-shunt electrodynamic metamaterial (EDMM) is assessed. It is demonstrated that the uncertainty can result in instabilities, and significant deviation from the desired resonance frequency and damping ratio. Avoiding instabilities requires the restriction of the shunt impedance to prevent uncertainties from resulting in a change in sign of the total circuit resistance, which in turn limits the ability to tune the device. The performance that can be achieved within these limitations is to

be investigated further, but a reduction in the variation in electrical parameters would significantly improve the ability to robustly tune the actuators in the presence of these uncertainties. Even with a limitation on the shunt impedance, designing an EDMM based on nominal actuator parameters can still result in instabilities in the presence of uncertainty, if actuators are tuned down in frequency. Therefore, the design must either restrict itself to only tuning the actuators up in frequency, or take into account uncertainties in the design.

## ACKNOWLEDGEMENTS

This research was partially supported by an EPSRC iCASE studentship (Voucher number 17100092) and the Intelligent Structures for Low Noise Environments (ISLNE) EPSRC Prosperity Partnership (EP/S03661X/1).

## REFERENCES

- [1] Hongwei Sun, Xingwen Du, and P. Frank Pai. Theory of Metamaterial Beams for Broadband Vibration Absorption. Journal of Intelligent Material Systems and Structures, 21(11):1085–1101, jul 2010.
- [2] Yong Xiao, Jihong Wen, and Xisen Wen. Broadband locally resonant beams containing multiple periodic arrays of attached resonators. Physics Letters A, 376(16):1384–1390, mar 2012.
- [3] R. Zhu, X.N. Liu, G.K. Hu, C.T. Sun, and G.L. Huang. A chiral elastic metamaterial beam for broadband vibration suppression. Journal of Sound and Vibration, 333(10):2759–2773, may 2014.
- [4] Hao Peng, P. Frank Pai, and Haoguang Deng. Acoustic multi-stopband metamaterial plates design for broadband elastic wave absorption and vibration suppression. International Journal of Mechanical Sciences, 103:104–114, nov 2015.
- [5] Graeme W Milton and John R Willis. On modifications of Newton’s second law and linear continuum elastodynamics. Proceedings of the Royal Society A: Mathematical, Physical and Engineering Sciences, 463(2079):855–880, mar 2007.
- [6] P. Frank Pai. Metamaterial-based Broadband Elastic Wave Absorber. Journal of Intelligent Material Systems and Structures, 21(5):517–528, mar 2010.
- [7] P. Frank Pai, Hao Peng, and Shuyi Jiang. Acoustic metamaterial beams based on multi-frequency vibration absorbers. International Journal of Mechanical Sciences, 79:195–205, 2014.
- [8] S. Behrens, A. J. Fleming, and S. O. Reza Moheimani. Electromagnetic shunt damping. In IEEE/ASME International Conference on Advanced Intelligent Mechatronics, AIM, volume 2, pages 1145–1150. Institute of Electrical and Electronics Engineers Inc., 2003.
- [9] Xinong Zhang, Hongpan Niu, and Bo Yan. A novel multimode negative inductance negative resistance shunted electromagnetic damping and its application on a cantilever plate. Journal of Sound and Vibration, 331(10):2257–2271, may 2012.
- [10] A J McDaid and B R Mace. A self-tuning electromagnetic vibration absorber with adaptive shunt electronics. Smart Materials and Structures, 22(10):105013, oct 2013.
- [11] E. Turco and P. Gardonio. Sweeping shunted electro-magnetic tuneable vibration absorber: Design and implementation. Journal of Sound and Vibration, 2017.
- [12] Emanuele Turco, Paolo Gardonio, Roberto Petrella, and Loris Dal Bo. Modular vibration control unit formed by an electromagnetic proof-mass transducer and sweeping RL-shunt. Journal of Vibration and Acoustics, 142(6):1–35, may 2020.
- [13] Tectonic Audio Labs. Tectonic TEAX09C005-8 Data Sheet. Technical report, 2020.
- [14] Dayton Audio. Dayton Audio DAEX-13-4SM Specification Sheet. Technical report, 2020.